

Reagentless, Electrochemical Aptasensor for Lead (II) Detection

Yan Lin, Lin Cheng, Guo Bing Wei, Ling Ling He, Cha Dan Chen, De Rong kong, Hong Peng* and Hao Fan†

Department of Pharmacy, Jiang Xi University of Traditional Chinese Medicine, Jiang Xi 330004, China

Received: November 01, 2016, Accepted: January 31, 2017, Available online: April 24, 2017

Abstract: A novel strategy for selective and sensitive amperometric detection of lead ion (Pb^{2+}) was proposed based on target-induced conformational switch. The ferrocene-labeled aptamer thiol was self-assembled through S-Au bonding on a gold electrode surface and the surface was blocked with 2-mercaptoethanol to form a mixed monolayer. The aptamer-modified electrode was characterized electrochemically by differential pulse voltammetry (DPV), and electrochemical impedance spectroscopy (EIS). The modified electrode showed a voltammetric signal due to a one-step redox reaction of the surface-confined ferrocenyl moiety of the aptamer immobilized on the electrode surface in 20mM Tris-HCl buffers buffer of pH 7.4. The “signal-on” upon Pb^{2+} association could be attributed to a change in conformation from random coil-like configuration on the probe-modified film to the quadruplex structure. The fabricated biosensor showed a linear response to the logarithm of Pb^{2+} concentration over the range of 5.0×10^{-10} M to 1.0×10^{-7} M with a detection limit of 1.2×10^{-10} M. In addition, this strategy afforded an exquisite selectivity for Pb^{2+} against other metal ions. The excellent sensitivity and selectivity show good potential for Pb^{2+} detection in real Chinese herb samples.

Keywords: Aptasensor, lead (II), electrochemical, reagentless

1. INTRODUCTION

Lead ions, which are one of the most toxic contaminants in aquatic ecosystems, pose a severe risk for human health and the environment [1]. Therefore, sensitive and on-site tracking of Pb^{2+} in aqueous media is of great importance in environmental and food monitoring, as well as clinical toxicology. Recent years have witnessed great progress in the development of optical sensors based on DNA [2–18], and most of them are focused on the lead dependent [8–17] DNAzyme [2–16], which can be combined with fluorophore/quencher pairs [2–10], nanoparticles [11–15] and other DNAzymes [16]. Compared to these optical assays, only a few electrochemical DNA sensors for Pb^{2+} detection were designed, which are still based on the Pb^{2+} -DNAzyme [19–21].

But the relatively high synthesis cost and low stability of Pb^{2+} specific DNAzyme limit its wide application. Alternatively, Pb^{2+} -induced allosteric G-quadruplex aptamers also can serve as specific Pb^{2+} sensing elements, with the conformational change being monitored by spectrometry, naked eyes or electrochemical methods [17-18, 22-24]. For example, Dong et al. developed a novel Pb^{2+} sensor with a G-quadruplex DNAzyme by colorimetry and

chemiluminescence (CL) [17]. Chang et al. reported thrombin-binding aptamer (G-rich DNA) for Pb^{2+} detection by fluorescence resonance energy transfer between a fluorophore and a quencher at the termini of each DNA probe [18].

Based on the results, the conclusion could be made that Pb^{2+} can sensitively and selectively react with G-rich single stranded DNA to form a G-quadruplex. Owing to the remarkable advantages of sensitivity, simplicity, low cost, rapid response and portability of electrochemical techniques, the development of electrochemical sensors for Pb^{2+} might hold great potential for facile pollutant monitoring [27]. To the best of our knowledge, there are two kind of electrochemical assay based on G-rich aptamer for Pb^{2+} detection have been reported [23, 25]. And they are both “signal-off” mode.

In a “signal-off” sensor, the mechanism is the alternation of distance of the labeled redox tags from the electrode by target DNA-induced conformational change of probe [26-27]. However, such “signal-off” sensors suffer from limited signal capacity, in which only a maximum of 100% signal suppression can be attained under any experimental conditions [28]. Moreover, such “signal-off” assays might cause false-positive results due to the coexistence of environmental stimulus [29-30].

In contrast, “signal-on” sensors can achieve much improved

To whom correspondence should be addressed:
Email: *516531260@qq.com, †fanhao11@aliyun.com
Phone: 0086-079187118923

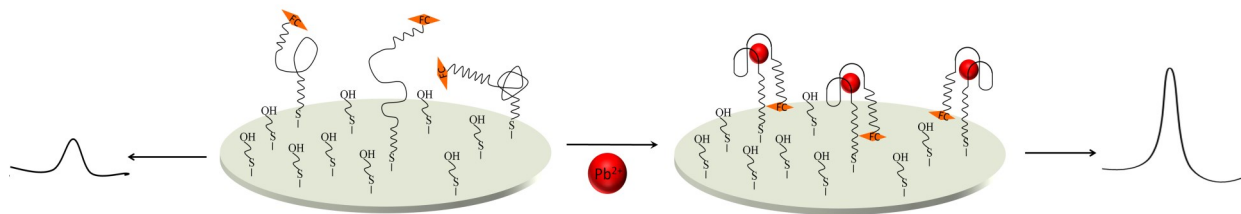


Figure 1. Schematic Conformation Representation of Aptamer on the Electrode Surface before (Coil-like) and after (Quadruplex) Aptamer- Pb^{2+} Association

signaling, and the background current observed in the absence of target is reduced, the gain of such a sensor, at least in theory, increases without limit [31-32].

Here, we report the development of a “signal-on” electrochemical Pb^{2+} aptasensor that combines the significant advantages of the electrochemical detection of a rapid and real-time monitoring of the biorecognition event with the versatility of reagentless surface-attached molecular beacons. This employs a bifunctionalized aptamer with a terminal electroactive ferrocene group as the reporter and the thiol function as the anchor on a gold electrode surface. The immobilized ferrocene-labeled aptamer showed a voltammetric signal due to a one-step redox reaction of the ferrocenyl moiety. Upon addition of Pb^{2+} , the duplex is induced to unwind while aptamer folds into the G-quadruplex structure stabilized by Pb^{2+} . As a result, the folded quadruplex structure due to target binding, significantly decreases electron-tunneling distance, bringing the ferrocene(Fc) label to the electrode surface and thus, enhancing the electron transfer. The selectivity and the practical application of the biosensor were also evaluated.

2. EXPERIMENTAL SECTION

2.1. Materials

2-Mercaptohexanol (2-ME) was purchased from Sigma-Aldrich. All metal salts used in this study (CaCl_2 , CoCl_2 , MgCl_2 , CuCl_2 , CdCl_2 , NiCl_2 , MnCl_2 , ZnCl_2 , AlCl_3 , and $\text{Pb}^{2+}(\text{NO}_3)_2$) were purchased from Sinopharm Chemical Reagent Co., Ltd. (Shanghai, China). Tris-HCl buffers were prepared by mixing stock standard solutions of Tris and HCl at various pH values. The aptamer sequences used in this work were purchased from the Takara Biotechnology Company (DaLian, China) as desalted products, and their sequences are listed below. Aptamer sequence: (5'-Fc-(CH_2)₆-GGTTGGTGTGGTTGG-SS-3')

Unless otherwise noted, all chemicals were purchased from Dingguo Biotechnology Inc. (Shanghai, China) and were of analytical reagent grade. All of the solutions were prepared with ultrapure water from a Millipore Milli-Q system. 0.1 M PBS (0.1M NaCl, 0.039 M NaH_2PO_4 , 0.061 M Na_2HPO_4 , pH 7.0), To reduce the S-S bonds and obtain the SH terminal groups, these products were treated with 10 mM Tris(2-Carboxyethyl) Phosphine Hydrochloride (TCEP, Sigma, Spain) for 1 h at room temperature. The aptamer-SH obtained was purified by passing through a Sephadex G25 column (NAP-10, Pharmacia Biotech). After elution with Milli-Q water, the concentration of the thiolated oligonucleotide was measured spectrophotometrically at 260 nm and subsequently stored at -20°C . Stock solutions of 5.5 μM oligonucleotide were stored at 4°C and diluted with 20mM Tris-HCl buffer (pH 7.4)

solution prior to use as needed for each specific experiment.

2.3. Electrochemical Measurements

All electrochemical measurements were performed with using an autolab electrochemical workstation (Metrohm Instruments Co., Swiss) in a one-compartment cell with a three-electrode system consisting of a modified gold working electrode, an Ag-AgCl reference electrode, and a platinum counter electrode in 5 mL of 20mM Tris-HCl buffers buffer (pH 7.4). Differential pulse voltammograms (DPVs) were registered in the potential interval -0.2 to +0.6 V vs Ag-AgCl, under the following conditions: modulation amplitude 0.05 V, step potential 0.001 V, and scan rate 0.002 V s⁻¹. Electrochemical impedance experiments were performed at the formal potential of attached ferrocene (E°) 0.165 V vs Ag/AgCl and an alternating potential ac with amplitude of 5 mV at the frequency range from 100 kHz to 100 mHz. A Nyquist plot (Z_{re} vs Z_{im}) was drawn to analyze the impedance results.

2.4. Probe Immobilization Procedure

Electrodes were cleaned by exposure to warm piranha solution for 1 h. [Piranha solution is a 1:3 (v/v) mixture of 30% H_2O_2 and concentrated H_2SO_4 . *Warning: This solution reacts Violently with organic materials and should be handled with great care.* The freshly cleaned gold electrodes (1.0 mm diameter) were incubated in a solution of 1×10^{-6} M HS-modified aptamer strand in 20mM Tris-HCl buffer (pH 7.4) for 2 h. Then the electrodes were washed with the buffer solution and subsequently incubated in 1 mM 2-mercaptohexanol for 1 h. The electrodes were then washed with Tris-HCl buffer and mounted into an electrochemical cell. After rinsing with the buffer, the electrodes were incubated for 30 min in a solution of $\text{Pb}(\text{NO}_3)_2$ in 20mM Tris-HCl buffers buffer (pH 7.4). The EIS of the films were recorded.

3. RESULTS AND DISCUSSION

3.1. Pb^{2+} induced DNA to G-quadruplex

The aptamer films were prepared by incubating freshly cleaned gold electrodes in solutions of 1×10^{-6} M aptamer, followed by backfilling potential pinholes and defects by soaking the film in 1 mM 2-mercaptohexanol in 20 mM Tris-HCl. This procedure prevents the molecules from laying flat on the surface and aligns the immobilized aptamer in an upright orientation. Then the modified electrodes were incubated in $\text{Pb}(\text{NO}_3)_2$ solution. In the presence of Pb^{2+} , aptamer formed the Pb^{2+} stabilized G-quadruplex as shown in Fig. 1. We then tested the feasibility of the proposed Pb^{2+} sensor by EIS in the form of a Nyquist plot (Figure 2). The equivalent circuit, as shown in the inset, was used to fit the EIS data. The components

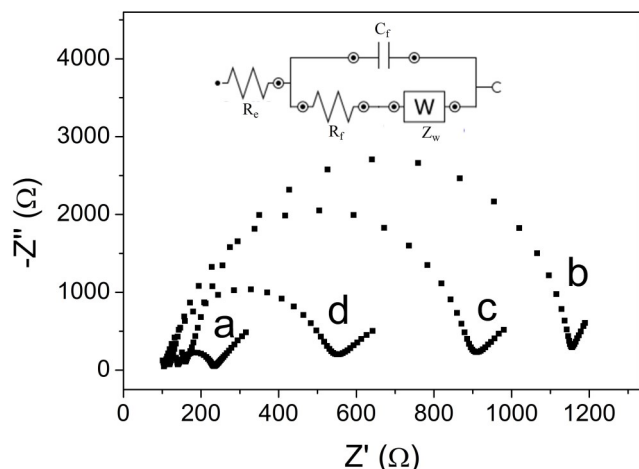


Figure 2. Nyquist plot for electrochemical impedance measurements in 0.01 mol/L PBS containing 0.01 mol/L $K_3[Fe(CN)_6]/K_3[Fe(CN)_6]$ (1:1) with amplitude of 5 mV at the frequency range from 100 kHz to 100 mHz: (a) bare Au electrode, (b) the thiolated aptamer modified Au electrode, (c) the aptamer and 2-ME modified Au electrode (d) the modified Au electrode after reacting with 1.0×10^{-7} M Pb^{2+} ions the hybridized electrode after. The inset is the equivalent circuit of the Nyquist plot.

in the equivalent circuit included the solution resistance (R_e), charge-transfer resistance (R_f), C_f related to double layer capacitance, and the Warburg impedance (Z_w). R_f of the electrode corresponds to the diameter of the semicircle in the Nyquist plot. As an ideal conductor, the bare gold electrode showed a small semicircle plot in the impedance spectra (Figure 2, curve a). After the modification of the aptamer, the electrode exhibited a much larger impedance (Figure 1, curve b). This is quite reasonable because the immobilization of aptamer on the gold electrode resulted in the highly negatively charged surface, reducing the electron transfer rate. After coadsorption of the small blocking agent 2-ME, the electrochemical impedance decreased to 800 ohm because the 2-ME effectively displaces the weaker adsorption contacts between aptamer nucleotides and the substrates, leaving the probe tethered primarily through the thiol end group. After the electrode was incubated with 1.0×10^{-7} Pb^{2+} , the electrochemical impedance decreased to 500 ohm due to the conformation of the aptamer change to G-quadruplex (Figure 1, curve d). The effect is to cause the approach of the redox label to the electrode surface, leading to significant decrease in the electron-transfer resistance.

3.2. Electrochemical behavior of Pb^{2+} detection

The electrochemical behavior of the immobilized 5'-Fc-aptamer-SH-3' was also investigated by differential pulse voltammetry (DPV). DPV is a pulse technique that allows much higher sensitivity than conventional sweep techniques when detecting very low concentrations of a redox probe. This is achieved by applying a small voltage pulse superimposed on the linear voltage sweep and sampling the differential current at a short time after the pulse. Hence, the measured current is only a product of the Faradaic process, with the capacitive charging current eliminated. Figure 3

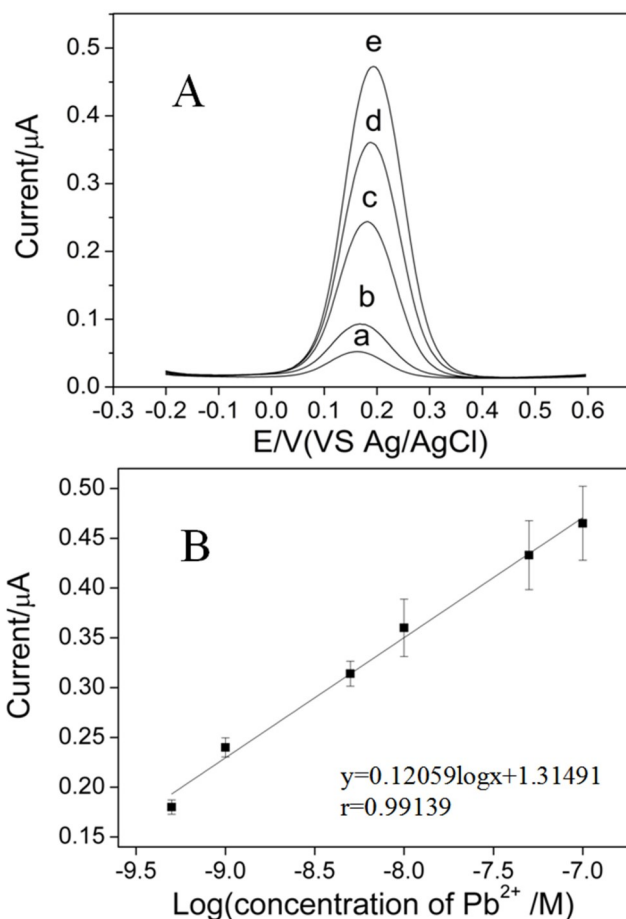


Figure 3. (A) Differential pulse voltammograms (DPVs) in blank 20 mM Tris-HCl buffer (pH 7.4) for (a) Fc-aptamer-coated Au electrode, (b) Fc-aptamer-2-ME-modified Au electrode (c) after exposure of Fc-aptamer-2-ME modified Au electrode to increasing concentrations of Pb^{2+} : 1.0×10^{-9} M, (d) 1.0×10^{-8} M, (e) 1.0×10^{-7} M, (modulation amplitude 0.05 V; step potential 0.001 V; scan rate 0.002 V s^{-1}). (B) The calibration plots of Pb^{2+} (5.0×10^{-10} to 1.0×10^{-7} M).

shows typical differential pulse voltammograms (modulation amplitude 0.05 V; step potential 0.001 V; scan rate 0.002 V s^{-1}) for Fc-aptamer/Au electrode with an anodic scan in Tris-HCl buffer of pH 7.4 (curve a). The peak of the Fc oxidation current shows increases after coadsorption of the small blocking agent 2-ME (curve b). The aptamer strand was primarily tethered through a sulfur-gold linkage with the presence of multiple contacts between each strand and the substrate [33]. The nucleotides can presumably adsorb to gold via multiple amines, as amines are known to adsorb weakly to gold surfaces [34]. The thiol group of the assembled 2-ME effectively displaces the weaker adsorption contacts between aptamer nucleotides and the substrates, leaving the probe tethered primarily through the thiol end group (Figure 1). Such conformation renders the probe to be more accessible to the target molecules. It is more likely that the nonspecific adsorption limits the flexibility of the chains and consequently hinders the diffusion of the redox probe

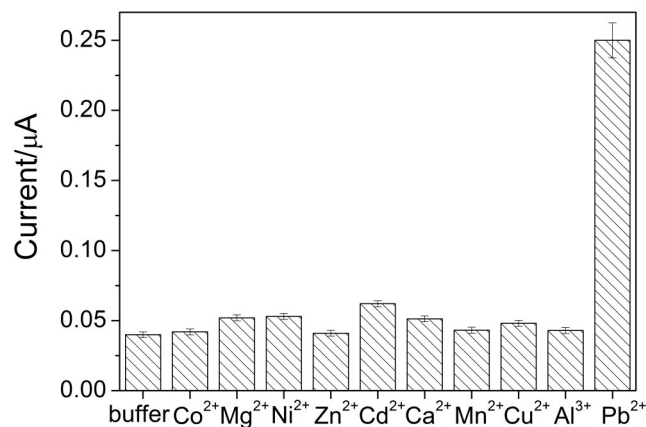


Figure 4. Selectivity of the proposed Pb²⁺ biosensor. The concentration of Pb²⁺ (1.0×10^{-9} M) and other metal ions are kept at 1.0×10^{-8} M.

toward the electrode surface. Moreover, the displacement of non-specific adsorption provides free volume into the film, which enhances the counteranions and solvent transport through the modified film. The anodic current signal increases after the addition of Pb²⁺ ion, Figure 3A (curve c-e), could be attributed to the conformation changes, which will shift the equilibrium toward the quadruplex structure, leading to an approach of the redox label to the electrode surface and the signal transduction is significantly enhanced between a linked label and the gold surface. The signal shows a slight shift to more anodic values, probably due to local medium effects on redox-active moiety. Polynucleotide strand conformations have previously been suggested to account for the electroactivity changes of an electroactive group tethered to a probe strand. As shown in Figure 3B, the anodic current signal increased for increasing concentration of Pb²⁺ ion dropped onto the electrode surface. The Fc oxidation signal shows a linear response with the Pb²⁺ concentration in the range 5.0×10^{-10} M to 1.0×10^{-7} M with a correlation coefficient of $r = 0.9913$. The low detection limit for Pb²⁺ was estimated to be 1.2×10^{-10} M.

The selectivity of the assay was also explored. The values of DPV were analyzed upon adding other metal ions (such as Co²⁺, Mg²⁺, Ni²⁺, Zn²⁺, Cd²⁺, Ca²⁺, Mn²⁺, Cu²⁺, Al³⁺) with the same concentration (1.0×10^{-8} M) instead of Pb²⁺ to the sensing system as shown in Fig. 4. Only Pb²⁺ caused a considerable anodic current increase while other ions yielded little changes in anodic current change, which indicated that response of the sensor to Pb²⁺ was unaffected by the presence of the most possible contaminating ions. Therefore, this simple electrochemical sensor based on DNA conformational switch is highly selective for Pb²⁺.

The practical use of the proposed biosensor was evaluated in Chinese herb (*Salvia miltiorrhiza* Bge) which was sampled from FangCheng of HeNan. The same sample was smashed to 100 mesh, drying at least 10 h in the oven of 120°C, 100 mL HNO₃ are added to the dried *Salvia miltiorrhiza* Bge (1g), then dissolved in the heating mantle, dropwise add H₂O₂ when the solution boiling up, stop when the solution turn transparent, concentrated to 20 mL as test solution.

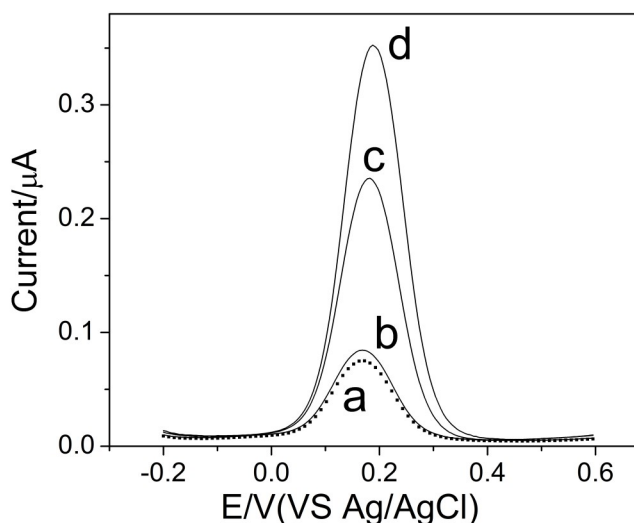


Figure 5. DPVs of the biosensor probe Pb²⁺ in *Salvia miltiorrhiza* Bge sample: blank sample (a), *Salvia miltiorrhiza* Bge sample (b), *Salvia miltiorrhiza* Bge sample + 1.0×10^{-9} M Pb²⁺ (c), *Salvia miltiorrhiza* Bge sample + 1.0×10^{-8} M Pb²⁺ (d).

The procedure was conducted for measurements by using *Salvia miltiorrhiza* Bge sample instead of Pb²⁺-containing buffer solution. Fc exhibited only a very small DPV signal increase (Fig.5 curve b), which is comparable to the original signal (Fig.5 curve a), indicating that the Pb²⁺ content in the tested sample is too low to be probed by the biosensor. However, there is an obvious current change in the readout signal if different concentrations of Pb²⁺ are added to the sample (Fig.5 curve c, d), indicating that the proposed biosensor can be applied for the analysis of Pb²⁺ in Chinese herb samples.

4. CONCLUSIONS

In conclusion, we have demonstrated an electrochemical aptasensor for the reagentless detection of a metal ion, Pb²⁺. The conformation change from coil-like to quadruplex structure upon association of aptamer with Pb²⁺ induces a significant increase in the Fc anodic current peak, thus facilitating a “switch on” detection. The reported sensor achieves impressive sensitivity and selectivity, with 1.2×10^{-10} M detection limits and negligible response to nonspecific metal ions being obtained. Based on these results, a simple, low-cost and label-free electrochemical biosensor for Pb²⁺ was constructed, which holds potential for Pb²⁺ in practical samples.

5. ACKNOWLEDGMENT

We gratefully acknowledge the financial support from the NSF of China (Grant No. 21265007, 81660658) and JiangXi Science and Technology Committee Foundation (Grant No. 20151512040663, 20161BAB215212), JiangXi Education Science Foundation (No. GJJ14610, GJJ14620).

REFERENCES

- [1] V. Meucci, S. Laschi, M. Minunni, C. Pretti, L. Intorre, G.

- Soldani, M. Mascini, *Talanta*, 77, 1143 (2009).
- [2] H. Wang, Y. Kim, H. Liu, Z. Zhu, S. Bamrungsap, W. Tan, J. Am. Chem. Soc., 131, 8221 (2009).
- [3] D.P. Wernette, C. Mead, P.W. Bohn, Y. Lu, *Langmuir*, 23, 9513 (2007).
- [4] J. Li, Y. Lu, *J. Am. Chem. Soc.*, 122, 10466 (2000).
- [5] J. Liu, A.K. Brown, X. Meng, D.M. Crokek, J.D. Istok, D.B. Watson, Y. Lu, *Proc. Natl. Acad. Sci. USA*, 104, 2056 (2007).
- [6] T. Lan, K. Furuya, Y. Lu, *Chem. Commun.*, 46, 3896 (2010).
- [7] J. Liu, Y. Lu, *Anal. Chem.*, 75, 6666 (2003).
- [8] C.B. Swearingen, D.P. Wernette, D.M. Crokek, Y. Lu, J.V. Sweedler, P.W. Bohn, *Anal. Chem.*, 77, 442 (2005).
- [9] X.B. Zhang, Z. Wang, H. Xing, Y. Xiang, Y. Lu, *Anal. Chem.* 82, 5005 (2010).
- [10] T.S. Dalavoy, D.P. Wernette, M. Gong, J.V. Sweedler, Y. Lu, B.R. Flachsbar, M.A. Shannon, P.W. Bohn, D.M. Crokek, *Lab. Chip*, 8, 786 (2008).
- [11] J. Liu, Y. Lu, *J. Am. Chem. Soc.*, 125, 6642 (2003).
- [12] J. Liu, Y. Lu, *J. Am. Chem. Soc.*, 126, 12298 (2004).
- [13] J. Liu, Y. Lu, *J. Am. Chem. Soc.*, 127, 12677 (2005).
- [14] Z. Wang, J.H. Lee, Y. Lu, *Adv. Mater.*, 20, 3263 (2008).
- [15] D. Mazumdar, J. Liu, G. Lu, J. Zhou, Y. Lu, *Chem. Commun.*, 46, 1416 (2010).
- [16] J. Elbaz, B. Shlyahovsky, I. Willner, *Chem. Commun.*, 1569 (2008).
- [17] T. Li, E. Wang, S. Dong, *Anal. Chem.*, 82, 1515 (2010).
- [18] C.W. Liu, C.C. Huang, H.T. Chang, *Anal. Chem.*, 81, 2383 (2009).
- [19] Y. Xiao, A.A. Rowe, K.W. Plaxco, *J. Am. Chem. Soc.*, 129, 262 (2007).
- [20] L. Shen, Z. Chen, Y. Li, S. He, S. Xie, X. Xu, Z. Liang, X. Meng, Q. Li, Z. Zhu, M. Li, X. C. Le, Y. Shao, *Anal. Chem.*, 80, 6323 (2008).
- [21] X. Yang, J. Xu, X. Tang, H. Liu, D. Tian, *Chem. Commun.*, 46, 3107 (2010).
- [22] C.L. Li, K.T. Liu, Y.W. Lin, H.T. Chang, *Anal. Chem.*, 83, 225 (2011).
- [23] Z. Lin, Y. Chen, X. Li, W. Fang, *Analyst*, 136, 2367 (2011).
- [24] E. Palecek, M. Fojta, *Anal. Chem.*, 66, 1566 (1994).
- [25] F. Li, L. Yang, M. Chen, P. Li, B. Tang, *Analyst*, 138, 461 (2013).
- [26] A.A. Lubin, K.W. Plaxco, *Acc. Chem. Res.*, 43, 496 (2010).
- [27] Q. Wang, L. Yang, X. Yang, K. Wang, L. He, J. Zhu, T. Su, *Chem. Commun. (Camb)*, 48, 2982 (2012).
- [28] F. Ricci, R.Y. Lai, K.W. Plaxco, *Chem. Commun.*, 3768 (2007).
- [29] A. Anne, A. Bouchardon, J. Moiroux, *J. Am. Chem. Soc.*, 125, 1112 (2003).
- [30] A.A. Lubin, R.Y. Lai, B.R. Baker, A.J. Heeger, K.W. Plaxco, *Anal. Chem.*, 78, 5671 (2006).
- [31] K.J. Cash, A.J. Heeger, K.W. Plaxco, Y. Xiao, *Anal. Chem.*, 81, 656 (2009).
- [32] Y. Xiao, A.A. Lubin, B.R. Baker, K.W. Plaxco, A.J. Heeger, *Proc. Natl. Acad. Sci. USA*, 103, 16677 (2006).
- [33] A.J. Bard, L.R. Faulkner, *Electrochemical Methods: Fundamentals and Applications*; John Wiley & Sons: New York, 1980.
- [34] D.V. Leff, L. Brandt, J.R. Heath, *Langmuir*, 12, 4723 (1996).